


Direct capture cross section of ${}^9\text{Be}(n, \gamma){}^{10}\text{Be}$

Peter Mohr*

Diakonie-Klinikum, Schwäbisch Hall D-74523, Germany
and Institute for Nuclear Research (Atomki), Debrecen H-4001, Hungary

 (Received 5 March 2019; revised manuscript received 19 April 2019; published 10 May 2019)

The cross section of the ${}^9\text{Be}(n, \gamma){}^{10}\text{Be}$ reaction was calculated in the direct capture model. All parameters of the calculations were adjusted to properties of the ${}^9\text{Be} + n$ system at thermal energies. The calculated cross section at thermonuclear energies shows the expected $1/v$ behavior of s -wave capture at low energies, but increases towards higher energies as typical p -wave capture. Excellent agreement between new experimental data in the astrophysically relevant energy region and the present calculation is found.

DOI: [10.1103/PhysRevC.99.055807](https://doi.org/10.1103/PhysRevC.99.055807)

I. INTRODUCTION

In a recent study the ${}^9\text{Be}(n, \gamma){}^{10}\text{Be}$ reaction was investigated at thermal and stellar energies [1]. The main aim of that study was the measurement of the cross section at energies in the keV region, which is essential to determine the astrophysical reaction rate at the high temperatures which can be found during core-collapse supernova explosions. Here the ${}^9\text{Be}(n, \gamma){}^{10}\text{Be}$ reaction may play an important role in the so-called α process under neutron-rich conditions [1].

In general, the formation of ${}^{12}\text{C}$ from nucleons and α particles is hindered by the gaps of stable nuclei at masses $A = 5$ and $A = 8$, which have to be bypassed by three-particle reactions. Depending on the α and neutron densities in the astrophysical environment, the triple-alpha ($\alpha\alpha\alpha$) process may be supplemented by the ($\alpha\alpha n$) or (αnn) reactions, which both proceed via ${}^9\text{Be}$, either directly produced in ($\alpha\alpha n$) or indirectly in (αnn) and subsequent ${}^6\text{He}(\alpha, n){}^9\text{Be}$. Then ${}^{12}\text{C}$ can be formed from the ${}^9\text{Be}(\alpha, n){}^{12}\text{C}$ reaction; however, ${}^9\text{Be}$ can also be detracted from the ${}^{12}\text{C}$ formation by either the ${}^9\text{Be}(n, \gamma){}^{10}\text{Be}$ or ${}^9\text{Be}(\gamma, n){}^8\text{Be}$ reactions (the latter becoming only relevant at high temperatures). The neutron-rich bypasses to the triple-alpha process occur in the α -process in core-collapse supernovae. The onset of the α -process is discussed in detail in Ref. [2], and further information on the relevance of the different three-body processes is given in Refs. [3,4].

Experimental data for the ${}^9\text{Be}(n, \gamma){}^{10}\text{Be}$ reaction in the keV region are very sparse. The resonance properties of the lowest resonance in ${}^9\text{Be}(n, \gamma){}^{10}\text{Be}$ have been studied by Kitazawa *et al.* [5], and three data points with relatively large error bars are provided by Shibata in an unpublished thesis made in the same group [6]. This gap is filled now by the new experimental data of Wallner *et al.* [1].

A very brief theoretical analysis of the new experimental data in the direct capture model is also given in Ref. [1], and it is concluded that the p -wave contribution had to be scaled down by about 30% to fit the new experimental data. It is the scope of the present study to provide a more detailed

analysis of the direct capture process in the ${}^9\text{Be}(n, \gamma){}^{10}\text{Be}$ reaction. It will be shown that the new data in the keV region can be well described if the parameters of the calculation are carefully chosen to reproduce the well-known properties of ${}^9\text{Be} + n$ at thermal energies (i.e., without any additional adjustment of parameters to the new data in the keV region). Furthermore, the contribution of low-lying resonances is re-analyzed, leading to a slightly different reaction rate at very high temperatures. Obviously, there is no major change in the astrophysical reaction rate at lower temperatures because finally the calculated p -wave contributions in Ref. [1] (adjusted to fit the new data in the keV region) and in this study (which fit the keV data without adjustment) are practically identical.

II. THE DIRECT CAPTURE MODEL

A. Basic considerations

As long as the level density in the compound nucleus (${}^{10}\text{Be}$ in the present case) is low, resonances play only a minor role, and the capture cross section is dominated by the direct capture (DC) process. Often this is the case for light nuclei, but DC may also be dominant for neutron-rich nuclei, in particular with closed neutron shells, where the low Q value of neutron capture corresponds to relatively small excitation energies and thus low level densities in the compound nucleus. As a nice example, DC was experimentally confirmed for the ${}^{48}\text{Ca}(n, \gamma){}^{49}\text{Ca}$ reaction [7], and it was possible to describe the cross section in the keV region after adjustment of the parameters to thermal properties of the ${}^{48}\text{Ca} + n$ system.

The full DC formalism is given by Kim *et al.* [8] and also listed in Refs. [7,9]. Basic considerations on DC were already by Lane and Lynn more than 50 years ago [10,11]. The chosen model in Ref. [1] is based on [12], which contains the same underlying physics with a focus on direct p -wave capture. Here I briefly repeat only the essential features of the DC model; for details, see [7–9,12].

The DC cross sections σ^{DC} scale with the square of the overlap integrals \mathcal{I} ,

$$\mathcal{I} = \int dr u(r) O^{E1/M1} \chi(r), \quad (1)$$

*mohr@atomki.mta.hu

TABLE I. Bound state properties of states in ^{10}Be below the neutron threshold. Energies E_x and spins and parities J^π are taken from [14]. The effective spectroscopic factors C^2S_{eff} of this study are defined in the text. Spectroscopic factors from transfer reactions are taken from the ENSDF database [20] and the compilation of Tilley *et al.* [14].

E_x (MeV)	E_B (MeV)	J^π	L	λ	C^2S_{eff}	$C^2S(d, p)$	$C^2S(\alpha, {}^3\text{He})$	$C^2S({}^7\text{Li}, {}^6\text{Li})$	$C^2S({}^8\text{Li}, {}^7\text{Li})$
0.0	-6.8123	0^+	1	1.1311	1.794	≈ 1.06	1.58	2.07	4.0
3.3680	-3.4443	2^+	1	0.9601	2.963	0.17	0.38	0.42	0.2
5.9584	-0.8539	2^+	1	0.7986	1.357	0.54	$< 0.73^a$		
5.9599	-0.8524	1^-	0	1.3492	0.523		$< 0.14^a$		
6.1793	-0.6330	0^+	1	0.7818	0.048				
6.2633	-0.5490	2^-	0	1.3084	0.467		0.08		

^aUnresolved.

where $\mathcal{O}^{E1/M1}$ is the electric or magnetic dipole operator; $E2$ transitions are much weaker than $E1$ transitions for the light $N \neq Z$ nucleus ^{10}Be and can be neglected for the DC calculations. The $u(r)$ and $\chi(r)$ are the bound state wave function and scattering state wave function. These wave functions are calculated from the two-body Schrödinger equation using a nuclear potential without imaginary part because the damping of the wave function in the entrance channel by the small DC cross sections is typically very small [13]. Finally, the DC cross section has to be normalized with the spectroscopic factor C^2S to obtain the capture cross section $\sigma_{\gamma,f}$ to a final state f :

$$\sigma_{\gamma,f} = (C^2S)_f \sigma_f^{\text{DC}}. \quad (2)$$

The total capture cross section σ_γ is obtained by the sum over all final states f :

$$\sigma_\gamma = \sum_f \sigma_{\gamma,f}. \quad (3)$$

An essential ingredient for the DC model is the nuclear potential $V(r)$ for the calculation of the wave functions $u(r)$ and $\chi(r)$. In the present work, a folding potential was used:

$$V(r) = \lambda V_F(r), \quad (4)$$

with the strength parameter λ of the order of unity. For details of the folding potential, see [7,9]. The advantage of the folding potential is that only one parameter, namely the strength λ , has to be adjusted, which reduces the available parameter space significantly (compared to the widely used Woods-Saxon potentials with three parameters).

B. Adjustment of the potential

For the calculation of bound state wave functions $u(r)$, the potential strength is adjusted to the binding energy of the respective state to ensure the correct asymptotic shape of $u(r)$. Thus, the only parameter λ of the potential is fixed for each final state f , and all wave functions $u(r)$ can be calculated without further adjustment of parameters (see Table I).

The scattering wave function $\chi(r)$ for the s wave with angular momentum $L = 0$ has to reproduce the thermal scattering length. From the bound coherent and incoherent scattering lengths $b_c = 7.79 \pm 0.01$ fm and $b_i = 0.12 \pm 0.03$ fm [15] it turns out that the free scattering lengths a_+ and a_-

for $J_+^\pi = 2^-$ and $J_-^\pi = 1^-$ are almost identical, and thus for simplicity a weighted average $\lambda = 1.4159$ was used for all scattering s waves instead of $\lambda_+ = 1.4097$ and $\lambda_- = 1.4263$. Note that the above J_+^π and J_-^π result from the coupling of the neutron spin $I_n^\pi = 1/2^+$, the spin of the ^9Be ground state $I_9^\pi = 3/2^-$, and angular momentum $L = 0$. The very minor variations of λ within about 1% do practically not affect the calculated DC cross sections.

The adjustment of the potential strength for the scattering p wave is more complicated because the thermal scattering lengths are related to s -wave scattering only. As an alternative, the same procedure as for the bound states was applied. Parameters λ were determined by adjustment to all bound ($E < 0$) and quasibound ($E > 0$) states in ^{10}Be where $L = 1$ transfer was clearly assigned in the $^9\text{Be}(d, p)^{10}\text{Be}$ or $^9\text{Be}(\alpha, {}^3\text{He})^{10}\text{Be}$ reactions [14]. From the average of all $L = 1$ states one finds a significantly lower $\lambda = 0.8856$ for the p wave, compared to $\lambda = 1.4159$ for the s wave. Similar to the s wave, the same value for λ was used for both channel spins J_+^π and J_-^π .

C. Adjustment of spectroscopic factors

Spectroscopic factors are required for neutron transfer to the $0p_{3/2}$, $0p_{1/2}$, and $1s_{1/2}$ shells. As the potential $V(r)$ is well constrained for the incoming s wave at thermal energies, spectroscopic factors C^2S can be derived from the thermal neutron capture cross section of ^9Be using Eq. (2).

The thermal neutron capture cross section has been determined in several experiments, and the results are in excellent agreement. I adopt $\sigma_\gamma = 8.299 \pm 0.119$ mb, which results from the weighted average of 8.27 ± 0.13 mb [16], 8.49 ± 0.34 mb [17], and 8.31 ± 0.52 mb from the new experiment [1]. The branching ratios to the individual final states in ^{10}Be are also taken from the recent experiment by Firestone and Revay [16].

For the bound states with $J^\pi = 2^+$, contributions of the transfers to the $0p_{3/2}$ and $0p_{1/2}$ shells have to be added. However, this can be simplified because the s wave capture scales approximately with $1/v$ for any combination of $0p_{3/2}$ and $0p_{1/2}$ transfer. As long as a proper adjustment to the capture cross section is made at thermal energies, the s -wave capture in the keV region must also be reproduced. Therefore, an effective spectroscopic factor C^2S_{eff} is listed in Table I,

which takes into account only the transfer to the $0p_{3/2}$ shell; contributions of the $0p_{1/2}$ transfer are neglected.

The adjustment of the effective spectroscopic factors to the thermal capture cross section is fortunately possible also for the 2^- state at $E_x = 6.263$ MeV because a weak M1 transition to this state was detected in Ref. [16]. Only for the 1^- state at $E_x = 5.960$ MeV an adjustment of C^2S from the thermal capture cross section is not possible because no primary γ ray could be detected. Consequently, C^2S for this state had to be fixed in a different way. For that purpose a procedure was used which relates the thermal scattering lengths to the spectroscopic factors of subthreshold s -wave states [18]. As the adjusted C^2S for the neighboring 2^- state from Eq. (2) is about 35% lower than C^2S from the procedure of [18], the same reduction factor was applied for the unknown C^2S for the 1^- state, leading to $C^2S = 0.523$ (see Table I). This value is roughly consistent with $C^2S \approx 0.4$, which can be derived with huge uncertainties from a weak secondary γ ray in thermal neutron capture after correction for feeding [16].

A comparison of the effective spectroscopic factors C^2S_{eff} in Table I to spectroscopic factors from transfer reactions like ${}^9\text{Be}(d, p){}^{10}\text{Be}$ is not straightforward. First, the effective spectroscopic factors of this study are calculated for the transfer to the $0p_{3/2}$ shell only, which simplifies the present calculations (see discussion above), but complicates the comparison to data from transfer reactions. Second, spectroscopic factors from transfer depend on the chosen parameters of the underlying calculations of the reaction cross sections [19], which are typically based on the distorted wave Born approximation (DWBA). This is reflected by wide variations of C^2S from (d, p) , $(\alpha, {}^3\text{He})$, and $({}^7\text{Li}, {}^6\text{Li})$. In some cases there is even disagreement on the transferred angular momentum L . The generally poor agreement of the C^2S from different transfer reactions is explicitly stated in the compilation of Tilley *et al.* [14]. Third, the two levels around $E_x = 5.96$ MeV in ${}^{10}\text{Be}$ cannot be resolved easily in transfer experiments. Therefore, I restrict myself here to list the adopted spectroscopic factors from different transfer reactions in Table I (as compiled in the ENSDF database [20] or given in Tilley *et al.* [14]). The only noticeable peculiarity is the deviation for the first excited 2^+ state in ${}^{10}\text{Be}$ between the huge $C^2S_{\text{eff}} \approx 3.0$ from the thermal (n, γ) cross section and $C^2S \approx 0.2$ – 0.4 from different transfer reactions. The thermal branching to the 2^+ state at $E_x = 3.368$ MeV is moderate with about 11%, but well defined [16], and thus C^2S_{eff} is well constrained in the present approach. A more detailed discussion of spectroscopic factors is omitted because of the significant uncertainties of the C^2S from the different transfer reactions.

III. RESULTS AND DISCUSSION

After the adjustment of the potential in Sec. II B and of the spectroscopic factors in Sec. II C, all parameters for the DC calculations are now completely fixed. The DC cross sections for s -wave and p -wave capture can now be calculated without any further adjustment of parameters. The results are shown in Fig. 1. As usual, s -wave capture decreases with energy by roughly $1/\sqrt{E}$, whereas p -wave capture increases with \sqrt{E} . A transition from the $1/\sqrt{E}$ to the \sqrt{E} behavior is found at

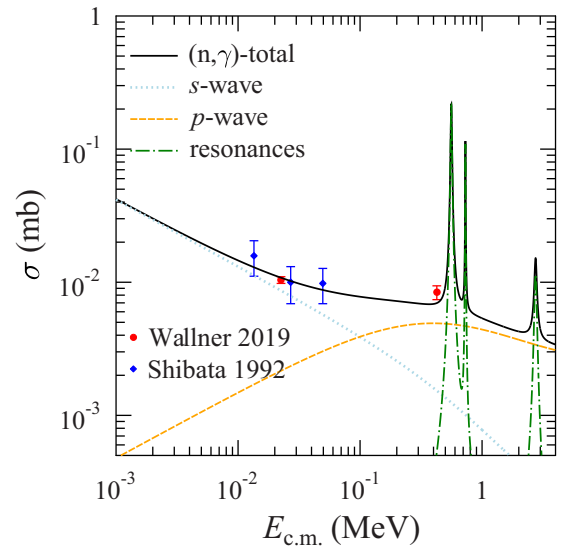


FIG. 1. Cross section of the ${}^9\text{Be}(n, \gamma){}^{10}\text{Be}$ reaction. The calculated total cross section (full black line) is composed of s -wave (light blue dotted) and p -wave (orange dashed) DC plus resonances (green dash-dotted). Excellent agreement with the experimental data [1,6] is found. For further discussion see text.

several tens of keV. This is a typical result for light nuclei at the upper end of the p -shell, like ${}^{12}\text{C}$ [21], and in the sd shell (e.g., ${}^{16}\text{O}$ [22,23] and ${}^{26}\text{Mg}$ [9]).

Important ingredients of the DC calculations like wave functions and overlaps are further illustrated in Fig. 2. Both bound state wave functions $u(r)$ [shown in the upper part (a) as $u^2(r)$ in logarithmic scale and in the middle part (b) as $u(r)$ in linear scale] of the 0^+ ground state and the 2^+ excited state at 5.96 MeV are characterized by $L_B = 1$ and thus mainly differ in the exterior, which is determined by the binding energies of both states. In contrast, the 1^- state at 5.96 MeV has $L_B = 0$ and one node in the interior. In the exterior, the 2^+ and 1^- wave functions show the same slope because of the almost identical binding energies.

The resulting integrand of the overlap integral in Eq. (1) is shown in the lower part (c) of Fig. 2 for a chosen energy $E = 100$ keV. Obviously, the main contributions for the capture to the ground state come from the nuclear interior and surface at relatively small radii ($r \lesssim 10$ fm). Because of the smaller binding energies of the 2^+ and 1^- final states, the main contributions for the transitions to these states appear in the nuclear exterior for radii $10 \lesssim r \lesssim 40$ fm. Nevertheless, for all transitions noticeable cancellation effects are found between the positive and the negative areas of the integrands in Fig. 2(c). A similar observation was already made in an earlier study of direct neutron capture at thermal energies [24], which is based on the model described in Ref. [25].

The DC calculation of s -wave and p -wave capture is complemented by the contributions of the four lowest known resonances, which correspond to the states in ${}^{10}\text{Be}$ at $E_x = 7.371$ MeV ($J^\pi = 3^-$), 7.542 MeV (2^+), 9.27 MeV (4^-), and 9.56 MeV (2^+). The properties of the resonances are listed in Table II.

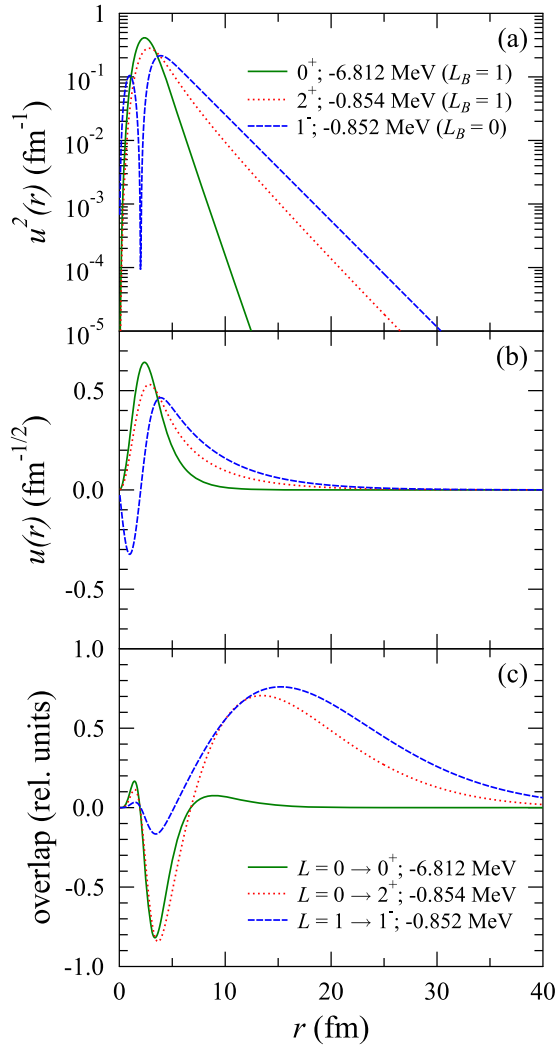


FIG. 2. Wave functions $u^2(r)$ [upper part (a), logarithmic scale] and $u(r)$ [middle part (b), linear scale] of the 0^+ ground state and the 2^+ and 1^- doublet of states at $E_x = 5.96$ MeV (see also Table I). The resulting integrand of the overlap integral in Eq. (1) is also shown for $E = 100$ keV [lower part (c)]. For further discussion see text.

For the calculation of the resonance cross sections the approximation $\Gamma \approx \Gamma_n$ was used because it is known that $\Gamma_\alpha/\Gamma_n \ll 0.1$ for these states [14]. The radiation width of the lowest resonance was determined experimentally as $\Gamma_\gamma = 0.73$ eV [5]. This 3^- resonance decays by $E1$ transitions to the first excited state in ^{10}Be ($\Gamma_\gamma = 0.62 \pm 0.06$ eV, which corresponds to a noticeable strength of 31 mW.u.) and to the second excited state ($\Gamma_\gamma = 0.11 \pm 0.08$ eV, corresponding to 124 mW.u.).

If one assumes the same average Weisskopf units for the $E1$ transitions in the decay of the next resonance with $J^\pi = 2^+$ at $E_x = 7.542$ MeV, one ends up with a smaller radiation width of $\Gamma_\gamma \approx 0.14$ eV because $E1$ transitions can only lead to odd-parity states around $E_x \approx 6$ MeV and thus correspond to relatively low transition energies. Because of the high transition energy of the $E2$ transition to the ground state, almost the same radiation width for the $E2$ transition can be estimated

TABLE II. Properties of low-energy resonances in the $^9\text{Be}(n, \gamma)^{10}\text{Be}$ reaction (taken from [14] except Γ_γ). The estimates of the radiative widths Γ_γ are explained in the text. All energies and widths are given in the c.m. system.

E_x (MeV)	E_R (MeV)	J^π	L	Γ (keV)	Γ_γ (eV)
7.371	0.559	3^-	2	15.7	0.73 ^a
7.542	0.730	2^+	1	6.3	0.28 ^b
9.270	2.458	(4^-)	2	150	1.3 meV ^b
9.56	2.748	2^+	1	141	2.43 ^b

^aExperimental value taken from [5].

^bEstimated from average radiation widths.

using a typical strength of about 5 W.u. for $E2$ transitions in this mass region [26]. This leads to an overall radiation width of $\Gamma_\gamma = 0.28$ eV, which is significantly lower than assumed by Wallner *et al.* who use the same $\Gamma_\gamma = 0.73$ eV as for the 3^- resonance.

Assuming the same strengths of 75 mW.u. for $E1$ and 5 W.u. for $E2$ transitions, the (4^-) resonance has only a tiny radiation width of $\Gamma_\gamma \approx 1.3$ meV, which results from the $E2$ transition to the 2^- state at $E_x = 6.263$ MeV. Additional γ transitions may occur to the levels in ^{10}Be above the neutron threshold with larger strength (e.g., for the $M1$ transition to the 3^- state at 7.371 MeV); however, the final state of this transition decays preferentially by neutron emission and thus does not contribute to ^{10}Be production.

A large radiation width is found for the 2^+ state at 9.56 MeV because of strong $E2$ transitions to low-lying 0^+ and 2^+ states in ^{10}Be : $\Gamma_\gamma \approx 2.43$ eV. However, this resonance is located at almost 3 MeV and thus contributes to the astrophysical reaction rate only at very high temperatures.

Interference effects between the resonances are not taken into account in the present study because no experimental information is available. However, it can be estimated that interference effects will be minor because the dominating 3^- d -wave resonance does not interfere with the dominating p -wave DC contributions.

For completeness it has to be noted that the two $L = 2$ resonances contain a significant amount of the total $L = 2$ strength. As these resonances are taken into account explicitly, an additional calculation of the d -wave contribution of the DC cross section would double count the $L = 2$ strength, and thus the d -wave contribution of the DC cross section is intentionally omitted. The folding potential for the s waves contains two $L = 0$ bound states close below the neutron threshold (see Table I). Assuming the same potential for the d wave automatically leads to the appearance of d -wave resonances at low energies, which are the theoretical counterparts of the experimentally observed d -wave resonances (see Table II).

Overall, the agreement between the calculated total cross section and the new experimental data [1] is very good, with a small $\chi^2 \approx 1.25$ per point. The dominating contribution to χ^2 comes from the upper data point at $E_{n,\text{lab}} = 473 \pm 53$ keV where an average cross section of $\sigma_{\text{exp}}^{\text{av}} = 8.4 \pm 1.0 \mu\text{b}$ is reported in Ref. [1]. The calculated cross section at exactly 473 keV is $\sigma_{\text{calc}} = 6.97 \mu\text{b}$. Averaging the calculated cross section

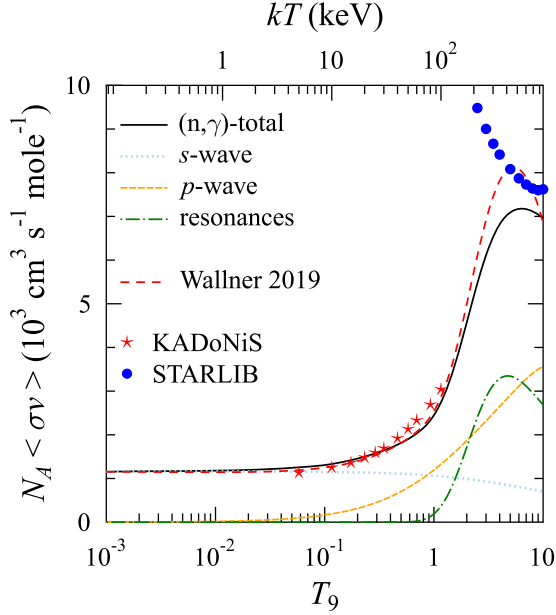


FIG. 3. Astrophysical reaction rate $N_A\langle\sigma v\rangle$ for the production of ${}^{10}\text{Be}$ in the ${}^9\text{Be}(n, \gamma){}^{10}\text{Be}$ reaction.

over the experimental energy distribution of the neutrons (see Fig. 3 of [1]) leads to $\sigma_{\text{calc}}^{\text{av}} = 7.18 \mu\text{b}$, which deviates only by 1.2σ from the experimental $\sigma_{\text{exp}}^{\text{av}}$. The increase from 6.97 to $7.18 \mu\text{b}$ results from the higher calculated cross sections at the upper end of the experimental neutron energy interval. As a consequence, χ^2 per point approaches 1.0 in this case. Including the Shibata points [6] reduces the deviations further to $\chi^2 \approx 0.6$ per point. It has to be repeated that the present calculation has been made completely independent, without any adjustment to the new experimental data points in the keV region.

IV. ASTROPHYSICAL REACTION RATE

The astrophysical reaction rate $N_A\langle\sigma v\rangle$ was calculated by numerical integration of the cross sections in Sec. III. A narrow energy grid from 1 to 4000 keV was used to cover the full temperature range up to $T_9 = 10$. Because of the relatively high first excited state in ${}^9\text{Be}$, no stellar enhancement factor was used (as also suggested in the KADoNiS database [27]). The result is shown in Fig. 3.

At low temperatures below a few keV this energy grid is not sufficient. Therefore, the calculation of the cross section was repeated in 10 eV steps from 10 eV to 50 keV. With these settings a constant rate for the s -wave capture was found down to the lowest temperatures in Fig. 3, which confirms that the numerical treatment is stable.

The s -wave capture dominates the low-temperature region below $T_9 \approx 0.1$, whereas at higher temperatures around $T_9 \approx 1$ p -wave capture becomes the major contributor. At even higher temperatures the resonance contributions become comparable to p -wave capture, which results mainly from the lowest 3^- resonance at 559 keV.

As expected, the present rate is in very good agreement with the rate by Wallner *et al.* [1] because their DC calculation was adjusted to their new experimental data (whereas the present calculation reproduces the new experimental data without adjustment). The only significant difference appears at relatively high temperatures around $T_9 \approx 5$ and results from the lower resonance strength of the lowest 2^+ resonance in the present study (see Table II and discussion in Sec. III). At the highest temperature $T_9 = 10$ in Fig. 3 the present rate becomes similar to the Wallner rate again because the lower strength of the 2^+ resonance is compensated by the additional resonances at higher energies which were not taken into account in Ref. [1].

Figure 3 also includes the recommended rate of the KADoNiS database [27] (version 1.0) which was derived from preliminary data of Wallner *et al.* and thus can be recommended for astrophysical calculations. The REACLIB database [28] also recommends to use the KADoNiS rate. However, STARLIB [29] contains a theoretical rate which is based on the statistical model. This theoretical rate exceeds the recommended rate by far at low temperatures and shows a completely different temperature dependence (see Fig. 3). Such a discrepancy is not very surprising because the statistical model is inappropriate for such light nuclei. A comparison of the new capture data to different libraries for neutron cross sections was already given in Ref. [1] and is omitted here.

The astrophysical reaction rate $N_A\langle\sigma v\rangle$ was fitted using the same parametrization as in Eq. (7) of [1]:

$$\frac{N_A\langle\sigma v\rangle}{\text{cm}^3\text{s}^{-1}\text{mol}^{-1}} = a_0(1.0 + a_1T_9^{1/2} + a_2T_9 + a_3T_9^{3/2} + a_4T_9^2 + a_5T_9^{5/2}) + a_6T_9^{-3/2} \exp(-b_0/T_9). \quad (5)$$

The a_i and b_0 parameters are listed in Table III. The deviation of the fitted rate is below 1% over the full temperature range.

V. CONCLUSIONS

The cross section of the ${}^9\text{Be}(n, \gamma){}^{10}\text{Be}$ reaction was calculated in the direct capture model. All parameters of the calculations could be adjusted to thermal properties of the ${}^9\text{Be} + n$ system, and therefore the calculation of the capture cross sections in the astrophysically relevant keV region is completely free of any adjustments. The calculated cross

TABLE III. Fit parameters a_i and b_0 of the recommended reaction rate $N_A\langle\sigma v\rangle_{\text{rec}}$ from Eq. (5).

a_0	a_1	a_2	a_3	a_4	a_5	a_6	b_0
1164.44	-0.062597	1.7712	-0.95285	0.22494	-0.021126	127297.1	6.64777

sections agree very well with the recently published experimental results by Wallner *et al.* [1] and also with earlier unpublished data by Shibata [6]. The astrophysical reaction rate of the KADoNiS database is essentially confirmed; it is based on a preliminary analysis of the Wallner *et al.* data. REACLIB also suggests to use the KADoNiS rate. However, the reaction rate of STARLIB should not be used because it is

based on a statistical model calculation which overestimates the experimental data significantly.

ACKNOWLEDGMENTS

I thank A. Wallner for encouraging discussions. This work was supported by NKFIH (K108459 and K120666).

-
- [1] A. Wallner, M. Bichler, L. Coquard, I. Dillmann, O. Forstner, R. Golser, M. Heil, F. Käppeler, W. Kutschera, C. Lederer-Woods, M. Martschini, A. Mengoni, S. Merchel, L. Michlmayr, A. Priller, P. Steier, and M. Wiescher, *Phys. Rev. C* **99**, 015804 (2019).
- [2] S. E. Woosley and R. D. Hoffman, *Astrophys. J.* **395**, 202 (1992).
- [3] J. Görres, H. Herndl, I. J. Thompson, and M. Wiescher, *Phys. Rev. C* **52**, 2231 (1995).
- [4] A. Bartlett, J. Görres, G. J. Mathews, K. Otsuki, M. Wiescher, D. Frekers, A. Mengoni, and J. Tostevin, *Phys. Rev. C* **74**, 015802 (2006).
- [5] H. Kitazawa, M. Igashira, S. Shibata, K. Tanaka, H. Takakuwa, and K. Masuda, *Nucl. Phys. A* **575**, 72 (1994).
- [6] S. Shibata, Ph.D. thesis, 1992 (unpublished), in Japanese.
- [7] H. Beer, C. Coceva, P. V. Sedyshev, Y. P. Popov, H. Herndl, R. Hofinger, P. Mohr, and H. Oberhummer, *Phys. Rev. C* **54**, 2014 (1996).
- [8] K. H. Kim, M. H. Park, and B. T. Kim, *Phys. Rev. C* **35**, 363 (1987).
- [9] P. Mohr, H. Beer, H. Oberhummer, and G. Staudt, *Phys. Rev. C* **58**, 932 (1998).
- [10] A. Lane and J. Lynn, *Nucl. Phys.* **17**, 563 (1960).
- [11] A. Lane and J. Lynn, *Nucl. Phys.* **17**, 586 (1960).
- [12] A. Mengoni, T. Otsuka, and M. Ishihara, *Phys. Rev. C* **52**, R2334 (1995).
- [13] E. Krausmann, W. Balogh, H. Oberhummer, T. Rauscher, K.-L. Kratz, and W. Ziegert, *Phys. Rev. C* **53**, 469 (1996).
- [14] D. Tilley, J. Kelley, J. Godwin, D. Millener, J. Purcell, C. Sheu, and H. Weller, *Nucl. Phys. A* **745**, 155 (2004).
- [15] V. F. Sears, *Neutron News* **3**, 26 (1992).
- [16] R. B. Firestone and Z. Revay, *Phys. Rev. C* **93**, 054306 (2016).
- [17] C. Conneely, W. Prestwich, and T. Kennett, *Nucl. Instrum. Methods Phys. Res., Sect. A* **248**, 416 (1986).
- [18] P. Mohr, H. Herndl, and H. Oberhummer, *Phys. Rev. C* **55**, 1591 (1997).
- [19] A. M. Mukhamedzhanov, F. M. Nunes, and P. Mohr, *Phys. Rev. C* **77**, 051601(R) (2008).
- [20] ENSDF database, <https://www.nndc.bnl.gov/ensdf/>, accessed 2019-01-26.
- [21] T. Ohsaki, Y. Nagai, M. Igashira, T. Shima, K. Takeda, S. Seino, and T. Irie, *Astrophys. J.* **422**, 912 (1994).
- [22] M. Igashira, Y. Nagai, K. Masuda, T. Ohsaki, and H. Kitazawa, *Astrophys. J., Lett.* **441**, L89 (1995).
- [23] P. Mohr, C. Heinz, M. Pignatari, I. Dillmann, A. Mengoni, and F. Käppeler, *Astrophys. J.* **827**, 29 (2016).
- [24] J. E. Lynn, S. Kahane, and S. Raman, *Phys. Rev. C* **35**, 26 (1987).
- [25] S. Raman, R. F. Carlton, J. C. Wells, E. T. Journey, and J. E. Lynn, *Phys. Rev. C* **32**, 18 (1985).
- [26] P. Endt, *At. Data Nucl. Data Tables* **55**, 171 (1993).
- [27] I. Dillmann, M. Heil, F. Käppeler, R. Plag, T. Rauscher, and F. Thielemann, in *Capture Gamma-Ray Spectroscopy and Related Topics: 12th International Symposium*, edited by A. Woehr and A. Aprahamian, AIP Conf Proc. No. 819 (AIP, New York, 2006), p. 123.
- [28] R. H. Cyburt, A. M. Amthor, R. Ferguson, Z. Meisel, K. Smith, S. Warren, A. Heger, R. D. Hoffman, T. Rauscher, A. Sakharuk, H. Schatz, F. K. Thielemann, and M. Wiescher, *Astrophys. J. Suppl. Ser.* **189**, 240 (2010).
- [29] A. L. Sallaska, C. Iliadis, A. E. Champagne, S. Goriely, S. Starrfield, and F. X. Timmes, *Astrophys. J. Suppl. Ser.* **207**, 18 (2013).